

A bio-imaging platform via Split-ring resonators microscopy

Yueh-Chun Lai¹, Hsin-Cheng Lee¹, Cheng-Kuang Chen¹, Ta-Jen Yen¹

¹Department of Materials Science and Engineering, National Tsing Hua University Hsinchu 30013, Taiwan, R.O.C.

Fax: + 886-3-5722366; email: tjyen@mx.nthu.edu.tw

Abstract

In this report, we built up a compact microscopic platform based on split-ring resonator (SRR). Owing advantages such as label-free, coupler-free, tunable spectrum range (from MIR to VIS) and longer detection length, the SRR microscopy (SRRM) is a strong competitor compared to the bulky surface plasmon resonance microscopy (SPRM) for biochemistry reaction detection in Bone marrow mesenchymal stem cells (BM-MSCs). Our experimental results has successfully demonstrated its capability of constructing the refractive index distribution images of BM-MSCs and meanwhile, obtaining the information of functional groups from the target cells. Therefore, we expect that the SRR microscopy (SRRM) delivers much simple optical configuration and better penetration depth for truly whole-cell imaging applications.

1. Introduction

The current prevailing technique of microscopy for bio-image is confocal microscopy, owing to its optimization for spatial resolution or high recording speed. Nevertheless, the confocal microscopy require fluorescent labeling, which may be detrimental to cells and more importantly, antibody binding to the surface antigens may affect the physiology of the cells by means of mechanotransduction. To overcome above issues, surface plasmon resonance microscopy (SPRM) that images the refractive index variations of local dielectric environment situated in the vicinity to the metal film emerges as powerful tool in a label-free fashion [1]. Moreover, it is a non-invasive method that does not require staining or labeling of the sample under examination and can minimize the alignment requirements for light coupling. However, the inherent issues in SPRM system such as demand of optical couplers (e.g., prisms and gratings), display of narrow operation ranges (typically at visible frequencies) and performance of short detection distances typically within a couple of hundreds of nanometers [2] destroys its integration with low-cost, real-time and high throughput biochips for rapid bio-analytical measurements of quantity-limited samples. To overcome these issues, here we present a compact microscopic platform based on split-ring resonator (SRR) or called “split-ring resonator microscopy (SRRM)” to substantially ease the burdens aforementioned (coupler-free, tunable spectrum range and longer detection length) and meanwhile to preserve the merit of the conventional SPRM technique (excellent sensitivity, label-free, quick and real-time diagnose, detection of refractive index variation).

Until today, the veiled physics of SRRs has become much clearer, for example, the spectral positions of multiple resonant reflectance peaks under normal incidence can be interpreted by our proposed standing-wave plasmonic resonances model (SWPR) [3]. More importantly, such a resonance condition depends on the local dielectric environment so sensitively that the SRRs can be readily employed as refractive-index (RI) sensors [4]. From our previous study [4], we manifested that the lower-order modes possess greater sensitivity associated with stronger localized electromagnetic field leading to shorter detection lengths within five hundreds nanometers, while the higher-order modes present mediate sensitivity with micron-scale detection lengths to allow intracellular bio-events detection. As a consequence, we build up an innovative label-free, coupler-free, multi-mode and tunable spectrum range microscopic platform based on the principles of plasmonic resonance of split-ring resonator (SRR) to observe bone marrow mesenchymal stem cells (BM-MSCs).

2. Split-ring resonators microscopy

The schematic of designed SRR pattern is shown in Fig. 1(a) through standard E-beam lithographic and lift-off processes. Transmission and reflection were characterized using a Fourier-transform infrared spectrometer combined with an infrared microscope. We used focal plane array detectors to image the sample as shown in Fig. 1(b). The intensity of the spectra is displayed in false color. We can find that the signal is strong within SRR region due to the fundamental plasmonic resonance of SRR and it can form pixel array in the infrared region. To observe the contrast of image, the resist PMMA was spin coated on the SRR samples and the result is shown in Fig. 1(c). By comparing with Figure 1(b) and 1 (c), obvious image contrast can be obtained in our platform successfully. Note that the main biochemical components as proteins, carbohydrates and waxes/lipids could be identified by their characteristic absorption from FT-IR imaging technique; however, our goal is use SRR resonance signal to identify the refractive index variation of bio-target so that we must carefully design the operated resonance frequency region of SRR to avoid overlap with the functional group signal of bio-target.

Figure 2(a) shows the reflectance spectra of BM-MSCs and its functional group signals of biochemical components are mainly at the wavelengths of $800\text{-}1800\text{ cm}^{-1}$ (Amide group) and $2800\text{-}3200\text{ cm}^{-1}$ (Lipid), respectively. Therefore, we fabricated SRR pattern on the quartz substrate whose fundamental resonance is within $1800\text{-}2800\text{ cm}^{-1}$ and the measured spectra are shown in Fig. 2(b). Next, bone marrow mesenchymal stem cells (BM-MSCs) were grown on top of the planar SRRs samples and quartz substrate as a control group, respectively. Figure 2(c) show the measurement spectra of BM-MSCs grown on the SRRs samples and it responds a significant red shift in multi-mode reflectance peaks compare with only SRRs sample due to variation of dielectric environment. Next, we used our proposed platform to construct bio-image of BM-MSCs based on the fundamental resonance signal (1st mode) of SRR at the wavenumber of $1700\text{-}2400\text{ cm}^{-1}$.

The left part of figure 2 (d) shows the resulting data for BM-MSCs. The main biochemical components as proteins, carbohydrates and waxes/lipids of BM-MSCs could be identified by their characteristic absorption. The distribution of biochemical components of BM-MSCs can be visualized by evaluating the intensity of the characteristic vibrations of each of these biochemical components. For examples, the IR images in the left part of figure 2(d) reveal the distribution of lipids within the BM-MSCs whose characteristic absorption are within $1200\text{-}1400\text{ cm}^{-1}$ and the IR images in the right part of figure 2(d) reveal no additional information because of none of characteristic absorption of BM-MSCs within $1800\text{-}2800\text{ cm}^{-1}$. Therefore, we use our SRR whose 1st resonance mode is at the wavenumber of $1800\text{-}2800\text{ cm}^{-1}$ to supply the refractive index distribution of BM-MSCs within this region. Figure 2(e) show the IR images of BM-MSCs grown on the SRRs samples by evaluating the intensity of the system at the wavenumber of $1800\text{-}2800\text{ cm}^{-1}$. Clearly, we can observe the refractive index distribution of BM-MSCs in our system. Due to plasmonic resonance, our SRR sensor can provide new contrast mechanism of microscopy that furnishes the detailed information on the BM-MSCs of the surface region of metallic pattern. Therefore, we can utilize the refractive index distribution information combining the functional group distribution of bio-target to analyze proliferation and differentiation process based on our SRR microscopy.

3. Figures

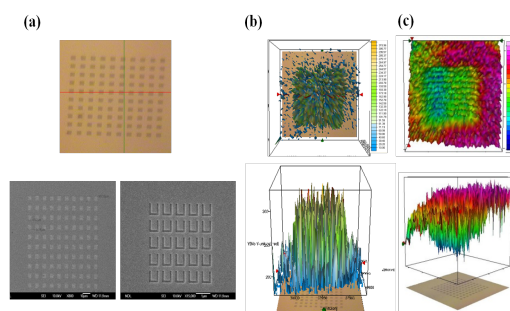


Fig. 1: (a) The OM and SEM images of fabricated planar SRRs and it consists of 5x5 SRR as a unit cell through standard E-beam lithographic and lift-off processes. (b) The fabricated SRR sample area and (c) fabricated SRR sample with spinning coat the PMMA on the surface has been measured in reflection mode with a pixel resolution of 2.7 μm using the FT-IR imaging system equipped with a focal plane array detector and a 15x objective (NA=0.4).

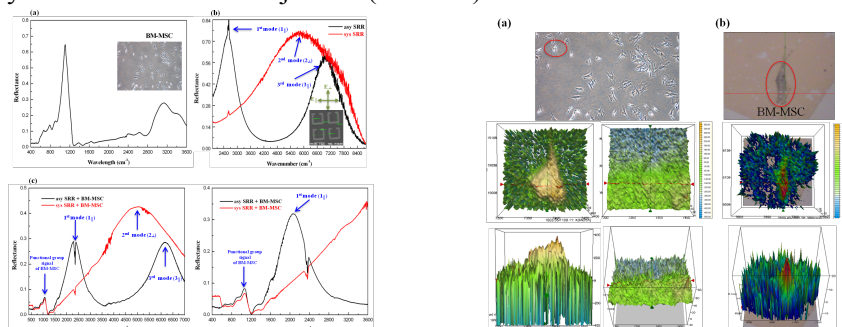


Fig. 2: (a) The normalized reflectance spectra of Bone marrow mesenchymal stem cells (BM-MSCs) and the inset shows its optical image. Its functional group signals of biochemical components are mainly at the wavelengths of 800-1800 cm^{-1} (Amide group) and 2800-3200 cm^{-1} (Lipid), respectively. (b) The normalized reflectance spectra of designed SRR sample and the inset shows its SEM picture. (c) The normalized reflectance spectra of designed SRR sample with BM-MSCs grown on surface. (d) The Bone marrow mesenchymal stem cells (BM-MSCs) sample area has been measured in reflection mode at the wavenumber 1200-1400 cm^{-1} (lipids; left part) and 1800-2800 cm^{-1} (no functional group; right part). (e) The designed SRR samples with BM-MSCs grown on surface sample area has been measured in reflection mode at the wavenumber 1800-2800 cm^{-1} . Obvious image contrast can be obtained by comparing with right part of fig2 (d).

4. Conclusion

In conclusion, we built up a compact microscopic platform based on split-ring resonator (SRR). Bone marrow mesenchymal stem cells (BM-MSCs) are the target to be observed in our platform. Deduced from the standing-wave plasmonic resonance model, we designed the resonance frequency of SRR at the wavenumber of 1800-2800 cm^{-1} without absorption from BM-MSCs. Our experimental results have successfully demonstrated its capability of constructing the refractive index distribution images of BM-MSCs and meanwhile, obtaining the information of functional groups from the target cells.

References

- [1] G. Steiner, "Surface plasmon resonance imaging," *Anal. Bioanal. Chem.* vol. 379, no. 3, pp. 328-331, 2004.
- [2] H. Raether, "Surface plasmons on smooth and rough surfaces and on gratings," Springer. 1988.
- [3] C. Y. Chen, S. C. Wu, and T. J. Yen, "Experimental verification of standing-wave plasmonic resonance in split-ring resonators," *Appl. Phys. Lett.* vol. 93, pp. 034110, 2008.
- [4] Y. T. Chang, Y. C. Lai, C. T. Li, C. K. Chen and T. J. Yen, "A multi-functional plasmonic biosensor," *Opt. Express.* vol. 18, no. 9, pp. 9561-9569, 2010.